

Permeability imaging using dynamic  
contrast enhanced MRI:  
validation with rat middle cerebral artery  
occlusion model

Hyun Seok Choi

Department of Medicine

The Graduate School, Yonsei University

Permeability imaging using dynamic  
contrast enhanced MRI:  
validation with rat middle cerebral artery  
occlusion model

Hyun Seok Choi

Department of Medicine

The Graduate School, Yonsei University

Permeability imaging using dynamic  
contrast enhanced MRI:  
validation with rat middle cerebral artery  
occlusion model

Directed by Professor Seung-Koo Lee

Doctoral Dissertation  
submitted to the Department of Medicine,  
the Graduate School of Yonsei University  
in partial fulfillment of the requirements for the degree  
of Doctor of Philosophy

Hyun Seok Choi

June 2013

This certifies that the Doctoral  
Dissertation of Hyun Seok Choi  
is approved.

-----  
Thesis Supervisor : Seung-Koo Lee

-----  
Thesis Committee Member#1 :

-----  
Thesis Committee Member#2 :

-----  
Thesis Committee Member#3 :

-----  
Thesis Committee Member#4 :

The Graduate School  
Yonsei University

June 2013

## ACKNOWLEDGEMENTS

I think it was God's blessing that I have met excellent colleagues and professors during my career as a student of medicine. It was also God's grace to accomplish the work and I think this has opened the door of my research. I would like to show gratitude for professor Seung-Koo Lee who has been my professor since I was a resident and has supervised my research. I also thank professor Ji Hoe Heo and Jae Hyoung Kim for teaching me so much about neurology and neuroradiology. Also, I thank professor Jong Eun Lee and Hye Yeon Lee for helping my researches; I had a great time working with them.

Also I give many thanks to Sei Young Kim for helping me achieve suitable and proper MR images. I thank Jungseok Yoo and Sung Soo Ahn who have accompanied me in the laboratory.

I send much love and thanks to my parents, who cheer me on with prayers, my beloved wife who always gives me strength, and to wonderful daughter Jimin, and my son Ji Hyuk who are the joy of my life.

June 2013

Hyun Seok Choi

# TABLE OF CONTENTS

ABSTRACT .....	1
I. INTRODUCTION .....	3
II. MATERIALS AND METHODS .....	4
1. Middle cerebral artery occlusion model .....	4
2. MRI acquisition .....	5
A. Dynamic contrast enhanced MRI .....	5
B. Diffusion weighted image .....	6
C. T2* weighted gradient echo image .....	6
3. Evans blue injection and brain extraction .....	7
4. Analysis of MRI .....	7
5. Analysis of specimen .....	8
6. Statistical analysis .....	9
III. RESULTS .....	9
1. Correlation analysis .....	11
2. Sequential changes of Ktrans after reperfusion .....	15
IV. DISCUSSION .....	17
V. CONCLUSION .....	19
REFERENCES .....	20
ABSTRACT(IN KOREAN) .....	25

## LIST OF FIGURES

Figure 1. Confirmation of acute infarct and hemorrhage .....	6
Figure 2. Selection of arterial input function for analysis of permeability parameters .....	8
Figure 3. Analysis of optical density .....	9
Figure 4. Extravasation of Evans and $K^{\text{trans}}$ map .....	10
Figure 5. Scatter plots and fitted linear regression lines of optical density versus permeability parameters .....	15
Figure 6. Sequential changes of $K^{\text{trans}}$ after reperfusion .....	16

## LIST OF TABLES

Table 1. Permeability parameters after analysis of DCE-MRI .....	12
Table 2. Results of Spearman's rho test .....	14
Table 3. Results of linear regression analysis .....	14
Table 4. . Sequential changes of $K^{\text{trans}}$ after reperfusion .....	16

<ABSTRACT>

Permeability imaging using dynamic contrast enhanced MRI:  
validation with rat middle cerebral artery occlusion model

Hyun Seok Choi

*Department of Medicine  
The Graduate School, Yonsei University*

(Directed by Professor Seung-Koo Lee)

Ischemic stroke is one of the most important leading causes of death in elderly patients. Microvascular permeability plays an important role not only in hemorrhagic transformation but also in the evolution of stroke. Previous studies using CT and MRI could not directly evaluate the interface of blood-brain barrier. Dynamic contrast enhanced MRI is a method of quantification of blood-brain barrier permeability. Recently, studies using MR permeability imaging have been reported more frequently in stroke research. The purpose of this study was to establish 3.0-Teslar MR sequence of permeability image and correlate MR images with findings of extravasation of Evans blue in the rat transient ischemia model. Sprague-Dawley rats with middle cerebral artery occlusion were imaged using 3.0-Teslar MRI with 8 channel wrist coil. Diffusion weighted images were used for the confirmation of acute infarct. Dynamic contrast enhanced MRI was performed 12hours, 18hours, and 36hours after reperfusion with intravenous injection of 0.2 mmol/kg gadolinium. Permeability parameters from DCE-MRI were calculated by Pride tools provided by Philips Medical System. 4 ml/kg of 2% Evan blue was injected after Dynamic contrast enhanced MRI and extravasation of Evans blue was correlated as a reference of integrity of blood brain barrier 10 hours after MRI. All permeability parameters ( $K^{\text{trans}}$ ,  $K_{\text{ep}}$ ,  $v_e$ , and  $v_e$ ) showed linear correlation with optical density of extravasation of Evans blue. The volume transfer constant ( $K^{\text{trans}}$ ) showed highest value of regression coefficient and correlation



coefficient (0.687 and 0.473 respectively,  $p < 0.001$ ). Changes in  $K^{\text{trans}}$  after reperfusion of MCA occlusion were mainly sequential increases in eight rats out of ten. However, there was one case with a sequential decrease and one with a stationary pattern. In conclusion, we established the MR sequence for permeability imaging and  $K^{\text{trans}}$  can provide information about later blood-brain barrier integrity.

---

Key words : stroke, dynamic contrast enhanced MRI, microvascular permeability

Permeability imaging using dynamic contrast enhanced MRI:  
validation with rat middle cerebral artery occlusion model

Hyun Seok Choi

*Department of Medicine  
The Graduate School, Yonsei University*

(Directed by Professor Seung-Koo Lee)

## I. INTRODUCTION

Ischemic stroke is one of the most important leading causes of death in elderly patients. Intravenous tissue plasminogen activator (t-PA) within three hours of onset has been proven to improve clinical outcome<sup>1</sup>. However, thrombolytic agents are associated with symptomatic intracerebral hemorrhage (ICH)<sup>2,3</sup>. Many efforts have been made to identify and predict hemorrhagic transformation in the field of stroke imaging. Among many independent risk factors of symptomatic ICH, hypodensity on computed tomography (CT) has been reported as an image-based risk factor<sup>3-7</sup>. There have also been studies using diffusion or perfusion weighted magnetic resonance images<sup>8-14</sup>. They showed the area of markedly decreased perfusion, decreased apparent diffusion coefficient, and reperfusion associated with hemorrhagic transformation. Although they showed promising results for predicting hemorrhagic transformation, their observations were not directly targeted at the interface of blood and brain. Permeability imaging enables the measurement of the blood-brain barrier's integrity<sup>15-22</sup>. Disruption of the blood-brain barrier (BBB) is not only associated with hemorrhagic transformation but also with the evolution of stroke. There may be activation of endothelium, production of free radicals, inflammation, cytokine

production, edema formation, and apoptosis. Microvascular permeability plays an important role in the pathologic process of stroke<sup>23-25</sup>. Recently, studies using MR permeability imaging have been reported more frequently in stroke research. Dynamic contrast enhanced MRI (DCE-MRI) is a method of quantification of BBB permeability, based on kinetic modeling of gadolinium based contrast agent in microvascular environment<sup>18,20,26</sup>. In-vivo MR imaging in stroke is important for understanding the mechanisms of stroke, establishing a therapeutic approach, and applying treatment to human subjects. Before clinical application, small animal models are indispensable for pre-clinical research. However, institutes with dedicated in-vivo animal MR systems and coils installed for animal research are limited. The purpose of this study was to establish a 3.0-Teslar MR sequence of permeability image and correlate MR images with findings of Evans blue extravasation in the rat transient ischemia model.

## II. MATERIALS AND METHODS

### 1. Middle cerebral artery occlusion model (MCAO model)

This animal study was approved by and performed in accordance with the institutional guidelines by Association for Assessment and Accreditation of Laboratory Animal Care International (AAALAC). Male Sprague-Dawley rats, 300-400 grams, were housed in an appropriate manner. The middle cerebral artery occlusion model was generated as described elsewhere with modifications<sup>27,28</sup>. In short, rats were anesthetized with intramuscular injection of mixture of Zoletil and Rompun (15 mg/kg and 10 mg/kg). Rectal temperature, respiration, and heart rates were monitored and maintained in the physiologic range throughout the procedure. The right common, internal, and external carotid arteries were exposed through a midline cervical incision. After ligation of the right common and external carotid arteries, 4-0 nylon monofilament whose tip was rounded by gentle heating was introduced via the right internal carotid artery to occlude the proximal middle cerebral artery, distal internal cerebral artery, and

anterior communicating artery. After an hour of transient occlusion of the middle cerebral artery, 4-0 nylon monofilament was removed to restore cerebral blood flow. A total of twenty one rats were included in this study. Initially twenty one rats were assigned to 3 groups, i.e., six rats to group 1; nine rats to group 2; and six rats to group 3. Four rats did not survive over the experimental schedule (n=1 in group 1; n=1 in group 2; and n=2 in group 3) and MCA occlusion failed to be made in two rats (n=1 in group 1 and n=1 in group 2).

## 2. MRI acquisition

Animal MR imaging was performed using a 3.0-Teslar system (Achieva, Philips, Best, the Netherlands) and 8-channel SENSE wrist coil. Rats were anesthetized with intramuscular injection of a mixture of Zoletil and Rompun (15 mg/kg and 10 mg/kg).

### A. Dynamic contrast enhanced MRI (DCE-MRI)

MRI acquisition was set at three time points: 12hours, 18hours, and 36hours after reperfusion. Twenty one rats were divided into three groups according to the number of MR acquisition: group 1, MR acquisition 12 hours after reperfusion; group 2, MR acquisition 12 hours and 18 hours after reperfusion; and group 3, MR acquisition 12 hours, 18 hours, and 36 hours after reperfusion. The tail vein was accessed and prepared for intravenous injection of contrast media before obtaining MR images. Dynamic contrast-enhanced MR images (DCE-MRI) were obtained after confirmation of acute infarct on diffusion weighted images (Fig 1a). Hemorrhagic transformation was evaluated by T2\* weighted gradient echo image (Fig 1b). For DCE-MRI, precontrast 3-dimensional T1-weighted images were obtained with the following parameters: FOV, 60x60 mm<sup>2</sup>; matrix, 112x112; slice thickness, 4.4 mm; slice increment, 2.2 mm; and flip angle of 5°. After precontrast scan, 60-dynamic contrast-enhanced T1-weighted images were taken with the same MR parameters except for a flip angle of 15° after bolus

injection of 0.2 mmol/kg gadolinium (Gadovist, Bayer, Berlin, Germany). Total scan time for dynamic contrast-enhanced MR images (DCE-MRI) was 4 minutes and 30 seconds. Fifteen rats were underwent DCE-MRI. Among them, two were excluded for analysis of DCE-MRI due to inappropriate contrast enhancement and suboptimal quality of images (n=1 in group 1 and n=1 in group 3). Therefore, thirteen rats were candidates for analysis of DCE-MRI.

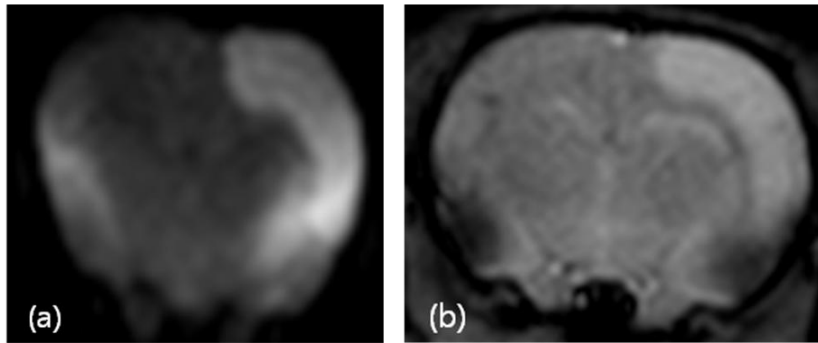


Figure 1. Confirmation of acute infarct and hemorrhage. (a) Diffusion weighted image ( $b=600 \text{ s/mm}^2$ ) showed confirmation of acute infarct in right cortex. (b) T2\* weighted gradient echo image showed no evidence of hemorrhagic transformation in right cortex.

#### B. Diffusion weighted image

Diffusion weighted images were acquired with the following parameters: FOV,  $60 \times 60 \text{ mm}^2$ ; matrix,  $128 \times 126$ ; slice thickness, 2 mm; and slice gap, 0.2 mm. Diffusion gradient was set at b-value of  $600 \text{ s/mm}^2$ .

#### C. T2\* weighted gradient echo image

T2\* weighted gradient echo image were acquired with the following parameters: FOV,  $60 \times 60 \text{ mm}^2$ ; matrix,  $192 \times 192$ ; slice thickness, 2 mm; and slice gap, 0.2 mm. There were no cases showing hemorrhagic transformation on T2\*

weighted gradient echo images.

### 3. Evans blue injection and brain extraction

Evans blue was injected immediately after the last MR acquisition. Using the venous route of tail vein, 4 ml/kg of 2% Evans blue (Sigma-Aldrich, St. Louis, MO, USA) in normal saline was injected. Anesthesia of lethal dose was performed 10 hours after the Evans blue injection. Rat brain was transcardially perfused with 4% paraformaldehyde. After brain extraction, the specimen was cooled in ice and then cut into 2-mm coronal sections. The posterior surface of each section was photographed by a digital camera.

### 4. Analysis of MRI

Permeability parameters were calculated by off-line Pride tools provided by Philips Medical System, which is based on the pharmacokinetic model of Tofts<sup>26</sup>. The two compartment model of Tofts assumes intravascular space and extravascular extracellular space, which is divided by the blood-brain barrier. The degree of contrast leakage from intravascular space to extravascular extracellular space is referred to as volume transfer constant ( $K^{trans}$ ). Reflux of contrast leakage from extravascular extracellular space to intravascular space is referred to as rate constant ( $K_{ep}$ ). Volume fraction of extravascular extracellular space is referred to as  $v_e$ . Volume fraction of plasma space is referred to as  $v_p$ . Those permeability parameters were calculated by means of iteration between time-intensity curves of artery and tissue in assumption of Tofts model<sup>26,28</sup>. Arterial input function was measured at the area of left internal carotid artery (Fig 2a) and its time-concentration curve was checked (Fig 2b). Two different regions of interest (ROIs) were placed in cortex and basal ganglia in ipsilateral and contralateral hemispheres of transient MCA occlusion. Because extravasation of Evans blue was prominent near the slices of Bregma-1.60 mm, they were targeted for analysis. Briefly, post-processing was composed of

motion correction of pixels from dynamic images, T1-mapping using different flip angles ( $5^\circ$  and  $15^\circ$ ), co-registration of pixels on T1-map, arterial input function estimation, and pharmacokinetic modeling. All these processes were automatically performed by Pride tools. Then, four types of permeability parameters ( $K^{\text{trans}}$ ,  $K_{\text{ep}}$ ,  $v_e$ , and  $v_p$ ) were calculated on each ROIs by Pride tools.

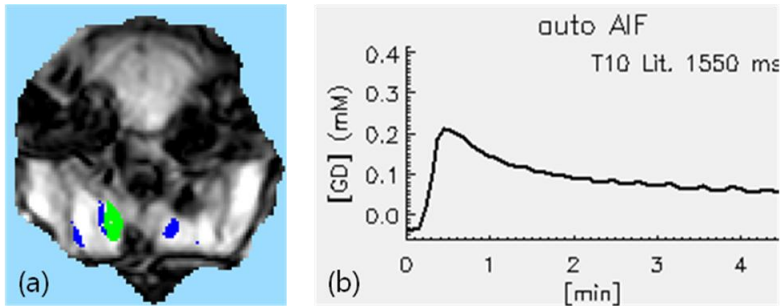


Figure 2. Selection of arterial input function (AIF) for analysis of permeability parameters. (a) Region of interest was set at region of left cervical internal carotid artery (green color). Venous flow was depicted in blue color. (b) Time-concentration of gadolinium curve showed rapid upslope and early peak of gadolinium concentration, suggestive of appropriate selection of arterial flow.

## 5. Analysis of specimen

The posterior surface of each section was photographed (Fig 3a). Photographs of posterior surface of Bregma-1.60 mm were loaded on Image J<sup>29</sup>. The photography of the specimen was split into three color channels: red, green, and blue. Because red channel images showed good contrast between normal appearing brain and leakage of Evans blue, red channel images were used for the analysis of optical density. Mean optical density was measured by ROIs in the ipsilateral cortex (Fig 3b) and basal ganglia (Fig 3c) along with contralateral cortex and basal ganglia. Optical density of corpus callosum was used for normalization of those ROIs. Normalized optical densities for each ROIs were calculated from each ROI divided by optical density of corpus callosum.

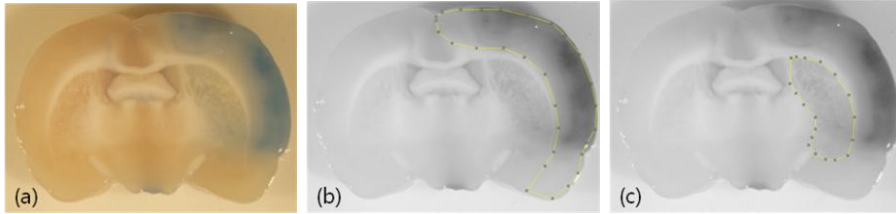


Figure 3. Analysis of optical density. (a) Posterior surface of sliced specimen (Bregma -1.60) was prepared for analysis of extravasation of Evans blue. ROIs were placed in right cortex (b) and basal ganglia (c) for measurement of optical density.

## 6. Statistical analysis

Correlation analysis was performed within each group and then regardless of groups. Scatter plots were drawn between optical densities and permeability parameters of each region of interest (ROI) regardless of groups. Optical density was considered as the dependent variable and permeability parameters were considered as the independent variables. The regression coefficient and the correlation coefficient were calculated. Fitted linear regression lines were calculated for each permeability parameters. Durbin-Watson statistic was calculated to assess normality and independence of residuals. Sequential changes of  $K^{\text{trans}}$  were described according to time points of MR acquisitions after reperfusion. For the statistical analysis we used the statistical software package, SPSS (version 20). Statistical significance was set at  $p < 0.05$ .

## III. RESULTS

Total of thirteen rats were finally successful for DCE-MRI and included for analysis (n=3 in group 1; n=7 in group 2; and n=3 in group 3). All thirteen rats showed acute infarct in right basal ganglia or cortex on diffusion weighted images.



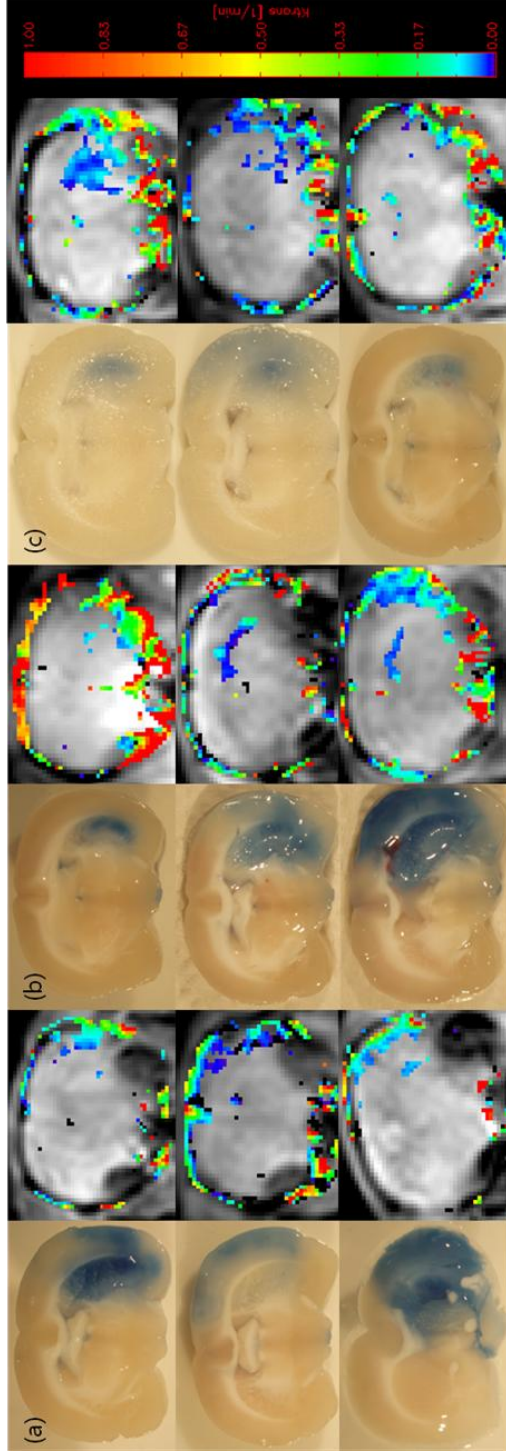


Figure 4. Extravasation of Evans blue and  $K^{trans}$  map. Extravasation of Evans blue was displayed on the left column and  $K^{trans}$  map on the right column in (a) 12 hours after reperfusion, (b) 18 hours after reperfusion, and (c) 36 hours after reperfusion.

## 1. Correlation analysis

DCE-MRI showed increase in permeability parameters in ipsilateral hemisphere of MCA occlusion (Table 1, Fig 4). There were no cases with a positive value of permeability parameters in contralateral normal-appearing hemisphere on DCE-MRI. Initially, correlation analysis was performed within groups. Because the number of samples were small from each group (n=12 in group 1; n=28 in group 2; and n=12 in group 3), nonparametric correlation analysis (Spearman's rho test) was performed. The results of Spearman's rho test showed all permeability parameters ( $K^{trans}$ ,  $K_{ep}$ ,  $v_e$ ,  $v_p$ ) from all 3 groups correlated with normalized optical density of extravasated Evans blue (Table 2). To evaluate correlation between permeability parameters and normalized optical density of extravasated Evans blue regardless of acquisition time after transient middle cerebral artery occlusion, Pearson correlation analysis was performed using ROI samples from all three groups (n=52). All the permeability parameters showed linear correlation with optical density (Table 3 and Fig 5). Among those permeability parameters,  $K^{trans}$  showed the highest value of regression coefficient and correlation coefficient (0.687 and 0.473 respectively,  $p < 0.001$ ). Durbin-Watson statistics for analysis of residuals showed 2.072, which was suggestive of normality and independence of residuals.

Table 1. Permeability parameters after analysis of DCE-MRI

Group	ROI	$K^{trans}$	$K_{ep}$	$v_e$	$v_p$	Optical Density	
1	IC	0.07	0.73	0.08	0.05	0.64	
	CC	0	0	0	0	0.96	
	IB	0.04	0.31	0.15	0.02	0.40	
	CB	0	0	0	0	1.03	
	IC	0.05	0.33	0.17	0.07	0.44	
	CC	0	0	0	0	0.98	
	IB	0.05	0.17	0.25	0.07	0.37	
	CB	0	0	0	0	1.03	
	IC	0.02	0.22	0.05	0.08	0.70	
	CC	0	0	0	0	0.97	
	IB	0.01	0.07	0.05	0.11	0.88	
	CB	0	0	0	0	1.02	
	2	IC	0.08	0.44	0.16	0.01	0.72
		CC	0	0	0	0	0.90
		IB	0.04	0.02	0.24	0.04	0.49
		CB	0	0	0	0	0.98
IC		0.08	0.57	0.15	0.09	0.44	
CC		0	0	0	0	0.91	
IB		0.04	0.44	0.09	0.03	0.40	
CB		0	0	0	0	1.00	
IC		0.06	0.8	0.07	0.04	0.66	
CC		0	0	0	0	0.92	
IB		0.05	0.27	0.29	0.06	0.56	
CB		0	0	0	0	0.98	
IC		0.02	0.16	0.5	0.05	0.93	
CC		0	0	0	0	0.98	
IB		0.08	0.34	0.32	0.05	0.93	
CB		0	0	0	0	0.98	
IC	0.07	0.48	0.15	0.01	0.83		

	CC	0	0	0	0	1.03
	IB	0.06	0.49	0.15	0.01	0.58
	CB	0	0	0	0	1.01
	IC	0.07	0.58	0.14	0	0.79
	CC	0	0	0	0	0.97
	IB	0.09	0.49	0.2	0.01	0.63
	CB	0	0	0	0	0.97
	IC	0.09	0.63	0.18	0.19	0.79
	CC	0	0	0	0	0.91
	IB	0.07	0.98	0.07	0.01	0.59
	CB	0	0	0	0	0.96
3	IC	0.06	0.8	0.07	0.04	0.93
	CC	0	0	0	0	0.97
	IB	0.05	0.28	0.2	0.06	0.80
	CB	0	0	0	0	1.01
	IC	0.04	0.5	0.1	0.12	0.77
	CC	0	0	0	0	0.97
	IB	0.03	0.16	0.68	0.1	0.74
	CB	0	0	0	0	1.01
	IC	0.01	0.02	0.02	0.09	0.90
	CC	0	0	0	0	0.93
	IB	0.04	0.21	0.17	0.08	0.73
	CB	0	0	0	0	0.99

Note: ROI refers to region of interest. IC, CC, IB, and CB refer to ipsilateral cortex, contralateral cortex, ipsilateral basal ganglia, and contralateral basal ganglia, respectively.

Table 2. Results of Spearman's rho test. The optical density was correlated with permeability parameters from each group

	Group 1		Group 2		Group 3	
	Correlation coefficient	P-value	Correlation coefficient	P-value	Correlation coefficient	P-value
$K^{trans}$ ( $\text{min}^{-1}$ )	-0.879	<0.001	-0.711	<0.001	-0.703	0.011
$K_{ep}$ ( $\text{min}^{-1}$ )	-0.832	0.001	-0.759	<0.001	-0.702	0.011
$v_e$	-0.927	<0.001	-0.668	<0.001	-0.858	<0.001
$v_p$	-0.722	0.008	-0.710	<0.001	-0.844	0.001

Table 3. Results of linear regression analysis.

	Regression coefficient	Correlation coefficient	Standard error of estimate	P-value	Durbin-Watson
$K^{trans}$ ( $\text{min}^{-1}$ )	0.687	0.473	0.145	<0.001	2.072
$K_{ep}$ ( $\text{min}^{-1}$ )	0.587	0.345	0.161	<0.001	2.281
$v_e$	0.471	0.222	0.176	<0.001	2.379
$v_p$	0.436	0.190	0.179	0.001	2.429

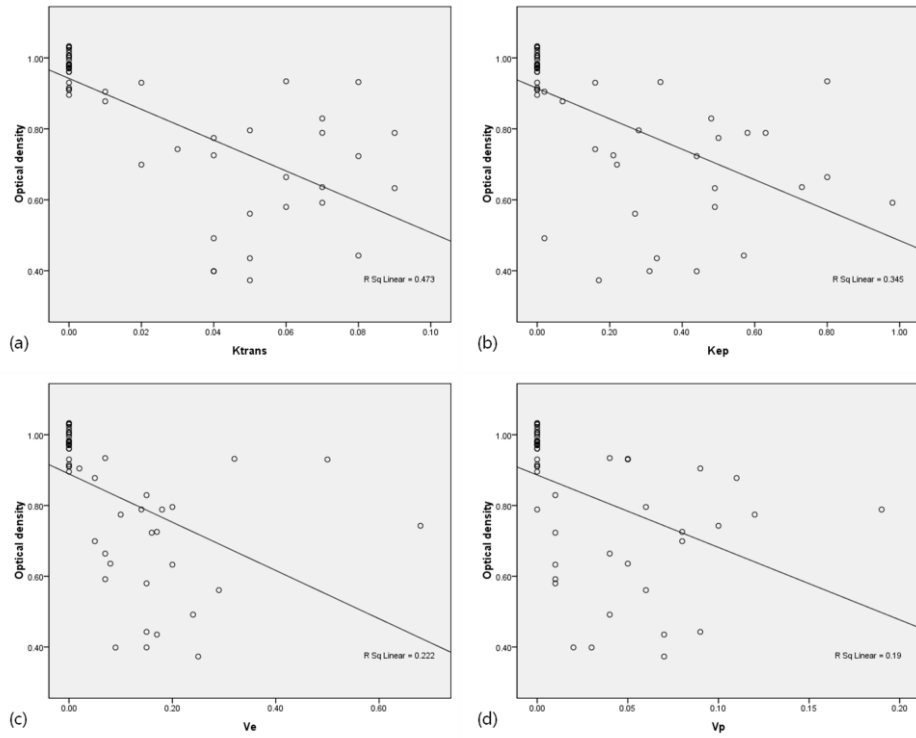


Figure 5. Scatter plots and fitted linear regression lines of optical density versus permeability parameters: (a)  $K^{trans}$ , (b)  $K_{ep}$ , (c)  $v_e$ , and (d)  $v_p$ .

## 2. Sequential changes of $K^{trans}$ after reperfusion

Area of extravasation of Evans blue showed variable pattern among rats from each group. Some showed dominant in basal ganglia and the other showed dominant both in basal ganglia and cortex (Figure 4). To evaluate pattern of changes in  $K^{trans}$  after reperfusion of MCA occlusion, average value of those in basal ganglia and cortex were used. Ten rats underwent multiple acquisitions of DCE-MRI, among which eight rats showed sequential increases of  $K^{trans}$ ; one showed a stationary value of  $K^{trans}$ , and one showed a sequential decrease of  $K^{trans}$  (Table 4 and Figure 6). The pattern of changes in  $K^{trans}$  were overall sequential increases in time.

Table 4. Sequential changes of  $K^{\text{trans}}$  after reperfusion. Average  $K^{\text{trans}}$  ( $\text{min}^{-1}$ ) of cortex and basal ganglia was listed in each cell.

Group	12-hour after reperfusion	18-hour after reperfusion	36-hour after reperfusion
1	0.055		
	0.050		
	0.015		
2	0.025	0.080	
	0.050	0.060	
	0.060	0.060	
	0.040	0.055	
	0.045	0.050	
	0.025	0.065	
	0.035	0.080	
3	0.030	0.045	0.055
	0.030		0.035
		0.030	0.025

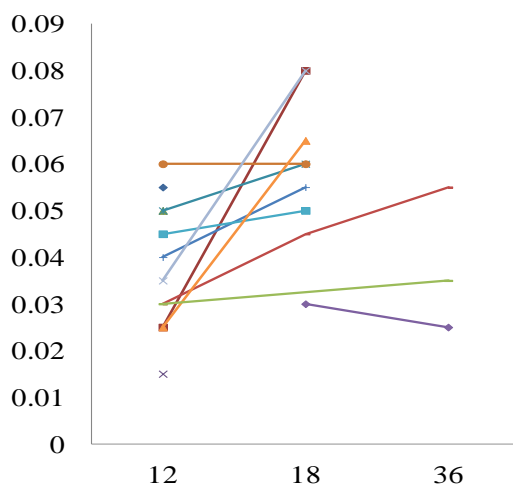


Figure 6. Sequential changes of  $K^{\text{trans}}$  after reperfusion. X-axis refers to hours after reperfusion and Y-axis refers to average  $K^{\text{trans}}$  ( $\text{min}^{-1}$ ) of cortex and basal ganglia.

#### IV. DISCUSSION

DCE-MRI is a method of quantification of blood-brain barrier permeability. DCE-MRI was recently developed advanced MR sequence which need high temporal and spatial resolution to detect changes in the microvascular environment. Previous results in animal models were usually performed using 4.7-, 7-Teslar, or higher Teslar animal-dedicated MR systems and coils<sup>30-35</sup>. In this study, we applied 3.0-Teslar MRI and 8-channel wrist coil to evaluate permeability in rat stroke model. Compared with previous studies with higher Teslar MR systems, our permeability images were inferior in voxel size and temporal resolution. However, all dynamic contrast enhanced MR images in our series were interpretable by means of the pharmacokinetic model of Tofts and correlated with later extravasation of Evans blue. All the rats showed increased permeability parameters in ipsilateral cortex or basal ganglia. DCE-MRI was consistent on predicting lateralization of later extravasation of Evans blue. However, in some cases, morphology and intensity of extravasation of Evans blue was different on visual inspection (Figure 4). Twelve hours of time interval between findings of Evans blue and DCE-MRI might be attributable for this discrepancy. Status of perfusion, reperfusion, collateral flow, and degree of ischemic insult were not evaluated on this study. Further verification on those factors should be performed in future study using homogeneous model of middle cerebral artery occlusion and shorter interval between brain extraction and MRI acquisition.

Our data showed that 4 types of permeability parameters were correlated with later extravasation of Evans blue. The most correlative parameter among them was the volume transfer constant. This result was consistent with previous studies, even though there was little difference in methodology of analysis<sup>32,33</sup>. Increased volume transfer constant detected 3 hours after embolic infarct was associated with progression in fibrin leakage<sup>32</sup>. Permeability parameters were sensitive to predict later hemorrhage as early as 3 hours after embolic infarct and volume



transfer constant is more sensitive than volume fraction of plasma space<sup>33</sup>. However, there were no cases with later hemorrhagic transformation in our data and therefore we could not evaluate permeability parameters for predicting later hemorrhage. No thrombolytic agent was used in this study design and this might partly explain no cases with later hemorrhagic transformation in our series.

The predominant pattern of sequential permeability changes in our data was a continuous increase in eight rats among ten rats which have 2 or more MR acquisitions. Two rats in our data showed different patterns: one stationary and the other a decrease in time. The two rats belong to group 3 and their permeability parameters were lower than those of group 1 or 2 at 12 hours and 18 hours after reperfusion (Table 4). Relatively weak extravasation of Evans blue was also noted from the rats in group 3 (Figure 4). Those might be explained by difference in severity of ischemic insult or pattern of BBB leakage after reperfusion. Previous studies have also reported a continuous pattern of BBB leakage after reperfusion<sup>30,31</sup>. However, there have been studies showing biphasic opening of the blood-brain barrier after a transient ischemia<sup>36,37</sup>. Controversies on this topic have been explained by the difference in stroke model, tracer characteristics, time points of MR acquisition, and analytical methods. Our data alone cannot explain the temporal dynamics of blood-brain brain in stroke evolution, and further research with more homogeneous model of middle cerebral artery occlusion is required on this topic.

Permeability parameters are quantifiable data which can be a candidate for imaging biomarkers for stroke treatment. Compared with histology-based methods, MRI-based methods are better for longitudinal study design. MRI enables repeated observation of single rat without sacrifice. Serial imaging during the whole experiment can eliminate inter-group variance, and therefore offer higher statistical power. Further research using DCE-MRI is necessary to provide information about BBB which can be applied to the clinical management of stroke.

Our study has a few limitations. Permeability change occurs in reperfused tissue after infarct. We did not evaluate the status of reperfusion, which can be

evaluated by MR angiography of perfusion weighted MRI. Status of reperfusion, timing of reperfusion, and status of collaterals may affect the result of permeability changes. In the case of failed reperfusion, gadolinium bolus may not reach the leaky vessels. This may result in underestimation of the volume transfer constant. Secondly, Evans blue extravasation was considered to be a reference standard to assess altered vascular permeability. However, the extent and density of permeability measured by MRI was different because there were innate differences in tracer characteristics in molecular weight, electric charge, and protein binding between gadolinium and Evans blue. In addition, there was a 10-hour interval between the last MR examination time and brain extraction time. The time interval between Evans blue injection and brain extraction was usually an hour or two in the previous studies. However, some of them used longer time intervals such as 24 hours<sup>38</sup>. In our study, permeability parameters from DCE-MRI can be predictive of Evans blue extravasation after 10 hours. Thirdly, there were no cases of gross hemorrhage in our experiment. This may have resulted from insufficient injury of BBB during MCA occlusion periods or no injection of thrombolytic agents.

## V. CONCLUSION

Permeability imaging using 3.0-Teslar MR system with wrist coil can provide information about contrast leakage in rat transient ischemia model. Permeability parameters were correlated with later Evans blue extravasation.  $K^{\text{trans}}$  showed the highest correlation coefficient among permeability parameters. Pattern of changes in  $K^{\text{trans}}$  after reperfusion of MCA occlusion were mainly sequential increases in time.

## REFERENCES

1. Tissue plasminogen activator for acute ischemic stroke. The National Institute of Neurological Disorders and Stroke rt-PA Stroke Study Group. *The New England journal of medicine* 1995;333:1581-7.
2. Lansberg MG, Albers GW, Wijman CA. Symptomatic intracerebral hemorrhage following thrombolytic therapy for acute ischemic stroke: a review of the risk factors. *Cerebrovascular diseases* 2007;24:1-10.
3. Tanne D, Kasner SE, Demchuk AM, Koren-Morag N, Hanson S, Grond M, et al. Markers of increased risk of intracerebral hemorrhage after intravenous recombinant tissue plasminogen activator therapy for acute ischemic stroke in clinical practice: the Multicenter rt-PA Stroke Survey. *Circulation* 2002;105:1679-85.
4. Intracerebral hemorrhage after intravenous t-PA therapy for ischemic stroke. The NINDS t-PA Stroke Study Group. *Stroke; a journal of cerebral circulation* 1997;28:2109-18.
5. Barber PA, Demchuk AM, Zhang J, Buchan AM. Validity and reliability of a quantitative computed tomography score in predicting outcome of hyperacute stroke before thrombolytic therapy. ASPECTS Study Group. *Alberta Stroke Programme Early CT Score. Lancet* 2000;355:1670-4.
6. Kase CS, Furlan AJ, Wechsler LR, Higashida RT, Rowley HA, Hart RG, et al. Cerebral hemorrhage after intra-arterial thrombolysis for ischemic stroke: the PROACT II trial. *Neurology* 2001;57:1603-10.
7. Larrue V, von Kummer RR, Muller A, Bluhmki E. Risk factors for severe hemorrhagic transformation in ischemic stroke patients treated with recombinant tissue plasminogen activator: a secondary analysis of the European-Australasian Acute Stroke Study (ECASS II). *Stroke; a journal of cerebral circulation* 2001;32:438-41.
8. Lansberg MG, Thijs VN, Bammer R, Kemp S, Wijman CA, Marks MP, et al. Risk factors of symptomatic intracerebral hemorrhage after tPA therapy for acute stroke. *Stroke; a journal of cerebral circulation* 2007;38:2275-8.

9. Alsop DC, Makovetskaya E, Kumar S, Selim M, Schlaug G. Markedly reduced apparent blood volume on bolus contrast magnetic resonance imaging as a predictor of hemorrhage after thrombolytic therapy for acute ischemic stroke. *Stroke; a journal of cerebral circulation* 2005;36:746-50.
10. Kim EY, Na DG, Kim SS, Lee KH, Ryoo JW, Kim HK. Prediction of hemorrhagic transformation in acute ischemic stroke: role of diffusion-weighted imaging and early parenchymal enhancement. *AJNR. American journal of neuroradiology* 2005;26:1050-5.
11. Hacke W, Albers G, Al-Rawi Y, Bogousslavsky J, Davalos A, Eliasziw M, et al. The Desmoteplase in Acute Ischemic Stroke Trial (DIAS): a phase II MRI-based 9-hour window acute stroke thrombolysis trial with intravenous desmoteplase. *Stroke; a journal of cerebral circulation* 2005;36:66-73.
12. Olivot JM, Mlynash M, Thijs VN, Kemp S, Lansberg MG, Wechsler L, et al. Relationships between infarct growth, clinical outcome, and early recanalization in diffusion and perfusion imaging for understanding stroke evolution (DEFUSE). *Stroke; a journal of cerebral circulation* 2008;39:2257-63.
13. Bang OY, Saver JL, Alger JR, Shah SH, Buck BH, Starkman S, et al. Patterns and predictors of blood-brain barrier permeability derangements in acute ischemic stroke. *Stroke; a journal of cerebral circulation* 2009;40:454-61.
14. Selim M, Fink JN, Kumar S, Caplan LR, Horkan C, Chen Y, et al. Predictors of hemorrhagic transformation after intravenous recombinant tissue plasminogen activator: prognostic value of the initial apparent diffusion coefficient and diffusion-weighted lesion volume. *Stroke; a journal of cerebral circulation* 2002;33:2047-52.
15. Lin K, Kazmi KS, Law M, Babb J, Peccerelli N, Pramanik BK. Measuring elevated microvascular permeability and predicting hemorrhagic transformation in acute ischemic stroke using first-pass dynamic perfusion CT imaging. *AJNR. American journal of neuroradiology* 2007;28:1292-8.
16. Hom J, Dankbaar JW, Soares BP, Schneider T, Cheng SC, Bredno J, et al. Blood-brain barrier permeability assessed by perfusion CT predicts symptomatic hemorrhagic transformation and malignant edema in acute ischemic stroke.

AJNR. American journal of neuroradiology 2011;32:41-8.

17. Lin K. Predicting transformation to type 2 parenchymal hematoma in acute ischemic stroke by CT permeability imaging. AJNR. American journal of neuroradiology 2011;32:E124; author reply E5.

18. Kassner A, Roberts T, Taylor K, Silver F, Mikulis D. Prediction of hemorrhage in acute ischemic stroke using permeability MR imaging. AJNR. American journal of neuroradiology 2005;26:2213-7.

19. Kassner A, Roberts TP, Moran B, Silver FL, Mikulis DJ. Recombinant tissue plasminogen activator increases blood-brain barrier disruption in acute ischemic stroke: an MR imaging permeability study. AJNR. American journal of neuroradiology 2009;30:1864-9.

20. Larsson HB, Courivaud F, Rostrup E, Hansen AE. Measurement of brain perfusion, blood volume, and blood-brain barrier permeability, using dynamic contrast-enhanced T(1)-weighted MRI at 3 tesla. Magnetic resonance in medicine : official journal of the Society of Magnetic Resonance in Medicine / Society of Magnetic Resonance in Medicine 2009;62:1270-81.

21. Thornhill RE, Chen S, Rammo W, Mikulis DJ, Kassner A. Contrast-enhanced MR imaging in acute ischemic stroke: T2\* measures of blood-brain barrier permeability and their relationship to T1 estimates and hemorrhagic transformation. AJNR. American journal of neuroradiology 2010;31:1015-22.

22. Warach S, Latour LL. Evidence of reperfusion injury, exacerbated by thrombolytic therapy, in human focal brain ischemia using a novel imaging marker of early blood-brain barrier disruption. Stroke; a journal of cerebral circulation 2004;35:2659-61.

23. Sandoval KE, Witt KA. Blood-brain barrier tight junction permeability and ischemic stroke. Neurobiology of disease 2008;32:200-19.

24. Wang CX, Shuaib A. Critical role of microvasculature basal lamina in ischemic brain injury. Progress in neurobiology 2007;83:140-8.

25. Dirnagl U, Iadecola C, Moskowitz MA. Pathobiology of ischaemic stroke: an integrated view. Trends in neurosciences 1999;22:391-7.

26. Tofts PS, Brix G, Buckley DL, Evelhoch JL, Henderson E, Knopp MV, et al. Estimating kinetic parameters from dynamic contrast-enhanced T(1)-weighted MRI of a diffusable tracer: standardized quantities and symbols. *Journal of magnetic resonance imaging : JMRI* 1999;10:223-32.
27. Ahn SK, Hong S, Park YM, Lee WT, Park KA, Lee JE. Effects of agmatine on hypoxic microglia and activity of nitric oxide synthase. *Brain Res* 2011;1373:48-54.
28. Kassner A, Mandell DM, Mikulis DJ. Measuring permeability in acute ischemic stroke. *Neuroimaging clinics of North America* 2011;21:315-25, x-xi.
29. Schneider CA, Rasband WS, Eliceiri KW. NIH Image to ImageJ: 25 years of image analysis. *Nature methods* 2012;9:671-5.
30. Durukan A, Marinkovic I, Strbian D, Pitkonen M, Pedrono E, Soenne L, et al. Post-ischemic blood-brain barrier leakage in rats: one-week follow-up by MRI. *Brain research* 2009;1280:158-65.
31. Strbian D, Durukan A, Pitkonen M, Marinkovic I, Tatlisumak E, Pedrono E, et al. The blood-brain barrier is continuously open for several weeks following transient focal cerebral ischemia. *Neuroscience* 2008;153:175-81.
32. Jiang Q, Ewing JR, Ding GL, Zhang L, Zhang ZG, Li L, et al. Quantitative evaluation of BBB permeability after embolic stroke in rat using MRI. *Journal of cerebral blood flow and metabolism : official journal of the International Society of Cerebral Blood Flow and Metabolism* 2005;25:583-92.
33. Ding G, Jiang Q, Li L, Zhang L, Gang Zhang Z, Ledbetter KA, et al. Detection of BBB disruption and hemorrhage by Gd-DTPA enhanced MRI after embolic stroke in rat. *Brain research* 2006;1114:195-203.
34. Taheri S, Candelario-Jalil E, Estrada EY, Rosenberg GA. Spatiotemporal correlations between blood-brain barrier permeability and apparent diffusion coefficient in a rat model of ischemic stroke. *PloS one* 2009;4:e6597.
35. Neumann-Haefelin C, Brinker G, Uhlenkuken U, Pillekamp F, Hossmann KA, Hoehn M. Prediction of hemorrhagic transformation after thrombolytic therapy of clot embolism: an MRI investigation in rat brain. *Stroke; a journal of cerebral circulation* 2002;33:1392-8.

36. Belayev L, Busto R, Zhao W, Ginsberg MD. Quantitative evaluation of blood-brain barrier permeability following middle cerebral artery occlusion in rats. *Brain research* 1996;739:88-96.
37. Pillai DR, Dittmar MS, Baldaranov D, Heidemann RM, Henning EC, Schuierer G, et al. Cerebral ischemia-reperfusion injury in rats--a 3 T MRI study on biphasic blood-brain barrier opening and the dynamics of edema formation. *Journal of cerebral blood flow and metabolism : official journal of the International Society of Cerebral Blood Flow and Metabolism* 2009;29:1846-55.
38. Kamada H, Yu F, Nito C, Chan PH. Influence of hyperglycemia on oxidative stress and matrix metalloproteinase-9 activation after focal cerebral ischemia/reperfusion in rats: relation to blood-brain barrier dysfunction. *Stroke; a journal of cerebral circulation* 2007;38:1044-9.

< ABSTRACT(IN KOREAN)>

역동적 조영 증강 MRI를 이용한 혈관투과도 측정:  
쥐 중뇌동맥 경색 모델을 이용한 검증

<지도교수 이 승 구>

연세대학교 대학원 의학과

최 현 석

뇌혈관장벽의 미세혈관투과도 변화는 급성 뇌졸중의 병태생리에 중요한 역할을 하는 것으로 알려져 있다. 최근에 역동적 조영증강 자기공명영상을 이용하여 미세혈관투과도를 정량적으로 측정하는 방법이 소개되었고, 동물을 이용한 뇌경색 연구에 사용되고 있다. 이 연구의 목적은 쥐를 이용한 중뇌동맥 경색 모델에서 역동적 조영증강 자기공명영상 획득 방법을 확립하고, 여기서 얻은 미세혈관투과도의 변화를 Evans blue 주입 후 조직 검체 소견과 비교하여 검증하는 것이다. Sprague-Dawley 쥐에서 미세필라멘트를 이용하여 우측 중뇌동맥을 1시간 폐쇄 후 재관류하여 경색 모델을 만들었으며, 확산강조 자기공명영상을 이용하여 뇌경색을 확인하였다. 역동적 조영증강 자기공명영상은 쥐의 꼬리 정맥에 0.2 mmol/kg의 가돌리늄 조영제를 주입한 후 얻었으며 실험군에 따라 경색 모델 후 12시간, 18시간, 36시간에 얻었다. 마지막 역동적 조영증강 자기공명영상을 얻은 후에 2% Evans blue 4 ml/kg를 쥐의 꼬리 정맥에 주입하였다.



조직 검체는 Evans blue 주입 후 10시간 후에 얻어서 사진 촬영하였다. 역동적 조영증강 자기공명영상에서 얻은 혈관 투과도와 조직 사진에서 얻은 Evans blue의 혈관외 유출을 Bregma-1.60 mm의 관심영역에서 측정하였다. 선형회귀분석을 이용하여 분석한 결과 역동적 조영증강 자기공명영상에서 얻은 혈관 투과도의 상관계수와 결정계수는 각각 0.687와 0.473이었다( $p < 0.001$ ). 경색 모델 후 18시간, 36시간에서의 혈관 투과도는 8마리에서 증가하는 양상을 보였지만, 감소하거나 변화 없는 양상을 보인 경우도 각각 1마리에서 있었다. 결론적으로, 본 실험에서 역동적 조영증강 자기공명영상 획득 방법을 확립하였으며, 이를 이용한 혈관투과도 측정은 뇌혈관장벽에 대한 예측적 정보를 제공해 주었다.

---

핵심되는 말 : 뇌졸중, 역동적 자기공명영상, 미세혈관투과도